iTRAQ-based proteomic analysis unveils ACSL4 as a novel potential regulator of human endometrial receptivity

Shuanggang Hu,[1]* Zhe Sun,[1]* Boyu Li,[1]* Hanting Zhao,[1] Yuan Wang,[1] Guangxin Yao,[1] Xinyu Li,[1] Xuejiao Bian,[1] Tin Chiu Li,[2] Hugo Vankelecom,[3] and Yun Sun[1#]

[1] Shanghai Key Laboratory for Assisted Reproduction and Reproductive Genetics, Center for Reproductive Medicine, Renji Hospital, School of Medicine, Shanghai Jiao Tong University, Shanghai 200135, China.

[2] Department of Obstetrics and Gynaecology, Chinese University of Hong Kong, Hong Kong, China

[3] Department of Development and Regeneration, Cluster Stem Cell Biology and Embryology, Research Unit of Stem Cell Research, University of Leuven (KU Leuven), B-3000 Leuven, Belgium

*** These authors contributed equally to this work.**

[#] **Corresponding author:** Yun Sun, M.D., Center for Reproductive Medicine, Renji Hospital, School of Medicine, Shanghai Jiaotong University, 845 Lingshan Road, Shanghai 200135, China (E-mail: syun163@163.com; Tel: 8621-20284500; ORCID ID: 0000-0002-7338-5541)

Keywords endometrial receptivity; implantation; proteome; iTRAQ; ACSL4

Financial Support

This work was supported by grants from the National Natural Science Foundation of China (No. 82130046, 81571435, 31900598, 82101747) , National Key Research and Development Program of China (No.2022YFC2702701, 2019YFA0802604), Shanghai leading talent program, Innovative research team of high-level local universities in Shanghai (No. SHSMU-ZLCX20210201, SSMU-ZLCX20180401), Clinical Research Plan of SHDC (SHDC2020CR1046B) , Shanghai Municipal Education Commission-Gaofeng Clinical Medicine Grant Support (No. 20161413) and Shanghai Jiaotong University School of Medicine Affiliated Renji Hospital Clinical Research Innovation Cultivation Fund Program (RJPY-DZX-003).

Disclosure Summary

The authors declare no conflict of interest.

Abstract

Competent endometrial receptivity is a prerequisite for successful embryo implantation. Identification of novel key molecules involved in endometrial receptivity is essential to better interpret human implantation and improve pregnancy rates in assisted reproduction treatment. The iTRAQ-based proteomics was performed to profile the proteomes of the prereceptive (LH+2, n=4) and receptive (LH+7, n=4) endometrial tissues. One hundred seventy-three differentially expressed proteins (DEPs) between LH+2 and LH+7 endometrial samples were identified. Integrated analysis of the proteomic data and published transcriptomic data was performed to identify the concordant DEPs with differential expression at both mRNA and protein levels. The protein-protein-interaction (PPI) network analysis were performed on concordant DEPs. We first identified 63 novel concordant DEPs and 5 hub proteins (ACSL4, ACSL5, COL1A1, PTGS1 and PLA2G4F) between LH+2 and LH+7 endometrial samples. ACSL4 was predominantly expressed in endometrial epithelial cells and its expression was significantly upregulated by progesterone in the LH+7 endometrium and significantly downregulated in repeated implantation failure (RIF) patients. Knockdown of ACSL4 in endometrial epithelial cells induced the down-regulation of endometrial receptivity markers (HOXA10, COX2 and LIF) and the significant decrease of implantation rate during in vitro implantation analysis. This study provides the first gel-independent quantitative proteomes of the LH+2 and LH+7 human endometrium using iTRAQ technology. The identified concordant DEPs and hub proteins open a new avenue for future studies aimed at elucidating the underlying mechanisms governing endometrial receptivity. ACSL4 was identified as a novel regulatory molecule in the establishment of endometrial receptivity and might play important roles during implantation.

Introduction

Successful implantation depends on high-quality embryos at the blastocyst developmental stage and optimal endometrial receptivity during the window of implantation, a temporally restricted period during which the endometrium in the mid-secretory phase (days 20-24 of the menstrual cycle) is receptive to embryo adhesion (1-3). Approximately two-thirds of implantation failures are reportedly caused by defective endometrial receptivity, whereas the embryo itself is responsible for only one-third of failures (2, 4). A significant proportion of couples undergoing IVF-ET (in vitro fertilization-embryo transfer) treatment experience RIF, which is usually defined as the absence of clinical pregnancy after transferring 6 top-quality embryos in at least three consecutive IVF cycles (5). Growing evidence suggests that endometrial receptivity defects are an important cause of RIF. Therefore, the regulatory mechanisms of endometrial receptivity urgently need clarification, which is fundamental for the understanding of human embryo implantation.

The establishment of reliable biomarkers for the detection of defects in endometrial receptivity has been a long-sought goal that remains an elusive target (6). With the rapid development of multiomics technologies, it has become possible to evaluate endometrial receptivity through transcriptome and proteome analysis, providing novel insights into potential markers of implantation (7). In recent decades, using cDNA microarrays and RNA-seq, comparative studies on transcriptomic profiles between the nonreceptive (proliferative and early secretory phases) and receptive (mid-secretory phase) endometrium have been performed to characterize specific gene expression patterns associated with endometrial receptivity (8-15). However, transcriptomic results do not necessarily represent the level of protein products due to posttranscriptional, translational, and posttranslational regulation related to cyclical transitions. Therefore, proteomics has also been increasingly used to clarify the protein expression changes between the nonreceptive and receptive human endometrium (16-25).

Multiple gel-based proteomic studies using two-dimensional gel electrophoresis (2-DE) or two-dimensional difference in-gel electrophoresis (DIGE) have identified several DEPs in the human endometrium across the cycle (Supplemental Table 1) (26). These include implantation-related proteins such as PGRMC1 and S100A10.

In 2015, using label-free technology, which is gel-independent, Chen *et al*. reported 317 DEPs between the proliferative and mid-secretory endometrium and uncovered energy metabolism and focal adhesion regulation responsible for endometrial receptivity (Supplemental Table 1) (21, 26).

Recently, the application of isobaric tags for relative and absolute quantitation (iTRAQ), a gel-free quantitative proteomics approach, greatly enhanced the comprehensive characterization of the proteomes of biological samples (27). iTRAQ, a label-based method, was developed for both relative and absolute quantitation using internal peptide standards. iTRAQ has the advantages of having a relatively high throughput and having relatively high sensitivity, high resolution, good reproducibility, easy automation and a wide detection range of protein abundance (27, 28). iTRAQ allows for the simultaneous analysis of up to eight samples in a single experiment, resulting in reduced analytical variability. To date, iTRAQ has been successfully employed to uncover the proteome of eutopic and ectopic endometriotic tissues (29) and to evaluate the effects of GnRH antagonists on endometrial protein profiles (30). However, until now, it has not been used to compare the protein expression levels between the prereceptive and receptive endometrium.

In this study, we used the iTRAQ method to characterize the proteomes of prereceptive and receptive endometrium and identify the DEPs that may be potential biomarkers for endometrial receptivity. To our knowledge, this is the first study to quantitatively unravel protein profiles in human prereceptive and receptive endometrium using a gel-independent method. We also for the first time performed an integrated analysis of transcriptomic and

proteomic data from prereceptive and receptive endometrial tissues and identified a concordant set of proteins with mRNA and protein expression changes. Additionally, ACSL4 was identified as a novel potential regulator of endometrial receptivity and potentially served as an etiological factor for RIF. This robustly advanced our understanding of complicated mechanisms governing endometrial receptivity.

Materials and Methods

Ethics statement

This study was approved by the Medical Ethics Committee of Renji Hospital, School of Medicine, Shanghai Jiaotong University. Written informed consent was obtained from all patients.

Human endometrial tissue samples

Human endometrial samples were collected using pipelle catheters under sterile conditions from women who underwent in vitro fertilization (IVF) or intracytoplasmic sperm injection (ICSI) at the Center of Reproductive Medicine at Renji Hospital. For the proteomic study, endometrial biopsy samples were retrieved from four women in the prereceptive (LH+2) phase and four women in the receptive (LH+7) phase, which was judged by the measurement of the urinary levels of LH. The average age of the eight women was 28.5 years, and the age range was between 22 and 35 years. An additional set of endometrial samples (proliferative phase, LH+2 and LH+7) was collected from different patients for the validation experiments. All abovementioned patients were diagnosed with tubal factor-related and/or male factor-related infertility. All of the patients had regular menstrual cycles and normal hormonal profiles and were free of uterine abnormalities. Another twenty-four endometrial samples during mid-secretory (LH+7) phase were collected from patients with male factor-related infertility (n=12) and patients with RIF (n=12). All endometrial samples were immediately frozen in liquid nitrogen after retrieval and stored at -80 °C until use.

Sample preparation

Frozen endometrial samples stored at -80 °C were ground into a fine powder in liquid nitrogen and lysed in SDS-lysis buffer (4% SDS, 0.1 M DTT, 0.1 M Tris-HCl, pH 8.0) with boiling at 100 ºC for 5 min, the homogenate was sonicated for 5 min on ice and centrifuged at 14,000×g for 40 min at 20 °C to remove cell debris. The protein concentration was determined using the BCA protein assay (Thermo Fisher Scientific, USA).

iTRAQ method

A total of 300 μg of protein from each sample was reduced, alkylated, and digested prior to labeling with iTRAQ reagent according to the manufacturer's instructions (AB Sciex, Framingham, MA). The iTRAQ labeling of peptides was performed using an iTRAQ Reagent-8plex Multiplex Kit (AB SCIEX, Framingham, USA) following the manufacturer's protocol. The digested peptides from prereceptive endometrium were labeled with tags 113, 114, 115 and 116, while the receptive group was labeled with tags 117, 118, 119 and 121. The eight labeled samples were pooled into one sample and dried in a vacuum centrifuge at room temperature. The iTRAQ-labeled peptides were subjected to high-pH reversed-phase fractionation by the 1100 Series HPLC Value System (Agilent, Palo Alto, USA) equipped with a Gemini-NX (Phenomenex, 00F-4453-E0) column (4.6×150 mm, 3 μm, 110 Å). The collected fractions (approximately 30) were finally combined into ten pools. Each fraction was concentrated via vacuum centrifugation and reconstituted in 40 μl of 0.1% v/v trifluoroacetic acid for liquid chromatography-tandem MS (LC–MS/MS) analysis. All of the samples were analyzed using Easy-nLC nanoflow HPLC system coupled with an Orbitrap Elite mass spectrometer (Thermo Fisher Scientific, San Jose, CA, USA). A total of 1 μg of each sample was loaded onto a peptide trap column (100 μm×2 cm, 5μm, 100 Å, C18, Thermofisher) at a flow rate of 150 nL/min using an autosampler with the same mass spectrometer setting as previously described (31).

Protein identification and quantification

All of the raw files were analyzed using the Proteome Discoverer 1.4 software (Thermo Electron, San Jose, CA). The following search parameters were applied: 1) monoisotopic masses, 2) trypsin digestion allowing for up to two missed cleavages, 3) fixed modifications: iTRAQ labeling and carbamidomethylation of cysteine, 4) variable modification: oxidation of methionine, 5) 0.05 Da tolerance for fragment ions, 10 ppm tolerance for precursor ions, and 6) peptide charges of +1, +2 and +3.

The results were filtered based on a false discovery rate (FDR) of no more than 1%. The quantitative protein ratios were weighted and normalized by the median ratio in Mascot (version 2.2, Matrix Science). When differences in protein expression between prereceptive and receptive groups were ≥1.5 (increased) or ≤0.67 (decreased), with $p < 0.05$, the protein was considered to be differentially expressed.

Bioinformatics analysis

A multiomics data analysis tool, OmicsBean (http://www.omicsbean.cn), was used to perform bioinformatic analysis of DEPs. The query proteins were linked to the Quick GO (Gene Ontology Analysis), KEGG Pathway (Pathway Analysis) and STRING (Protein–Protein Interaction Analysis) databases for downstream analysis.

Real-time RT–PCR

Total RNA was extracted from human endometrial tissues with TRIzol (Invitrogen, Grand Island, USA) according to the manufacturer's instructions. Total RNA (1 μg) was used to synthesize cDNA using a first-strand cDNA synthesis kit (Toyobo) according to the manufacturer's instructions. Real-time PCR was performed using SYBR Green master mix (Toyobo) with a Rotor-Gene 6000 machine (Corbett Research, Sydney, Australia). The primers were as follows: ACSL4: 5'CATCCCTGGAGCAGATACTCT3' (forward), 5'TCACTTAGGATTTCCCTGGTCC3' (reverse); β-actin:

5‘CATGTACGTTGCTATCCAGGC3’ (forward), 5’CTCCTTAATGTCACGCACGAT3’ (reverse).

Western blot

Western blot analysis was conducted following a previously described protocol (32). Briefly, proteins were separated by SDS–PAGE and blotted onto nitrocellulose membranes. The membranes were incubated with primary antibodies against ACSL4 (1:250; Santa Cruz Biotechnology Cat# sc-365230, RRID:AB_10843105, http://antibodyregistry.org/AB_10843105), HOXA10 (1:500; Santa Cruz Biotechnology Cat# sc-17158, RRID:AB_2248649, http://antibodyregistry.org/AB_2248649), COX2 (1:1000; Cell Signaling Technology Cat# 12282, RRID:AB_2571729, http://antibodyregistry.org/AB_2571729), LIF (1:500; Abcam Cat# ab113262, RRID:AB_10861387, http://antibodyregistry.org/AB_10861387), and β-actin (1:10000; Proteintech Cat# 66009-1-Ig, RRID:AB_2687938, http://antibodyregistry.org/AB_2687938) or GAPDH (1:10000; Proteintech Cat# 60004-1-Ig, RRID:AB_2107436, http://antibodyregistry.org/AB_2107436) overnight at 4°C. The membranes were washed and incubated with horseradish peroxidase (HRP)-conjugated goat anti-rabbit IgG(1:10000; Proteintech Cat# SA00001-2, RRID:AB_2722564, http://antibodyregistry.org/AB_2722564), HRP-conjugated goat anti-mouse IgG (1:10000; Proteintech Cat# SA00001-1, RRID:AB_2722565, http://antibodyregistry.org/AB_2722565) or HRP-conjugated rabbit anti-goat IgG (1:10000; Proteintech Cat# SA00001-4, RRID:AB_2864335, http://antibodyregistry.org/AB_2864335) for 1h and visualized using an enhanced chemiluminescence detection system (Millipore, USA).

Immunohistochemistry

Human endometrial tissue samples were fixed in 4% paraformaldehyde and embedded in paraffin. Immunohistochemical staining of endometrial sections was performed using ACSL4

antibody (1:100, Santa Cruz) overnight at 4 °C. The sections were washed and incubated with secondary antibody conjugated with horseradish peroxidase (HRP) for 1 h at room temperature. As a negative control, serial sections were subjected to the same procedure, with normal rabbit serum replacing the primary antibody. The endometria were counterstained with Harris hematoxylin.

Knockdown of ACSL4 in Ishikawa cells

The ACSL4 shRNA was designed based on the Sigma shRNA library (www.sigmaaldrich.cn/CN/zh/semi-configurators/shrna), and the sequences of scramble and shACSL4 were as follows: shACSL4: CCTCAAAGACATTGAACGAAT (5'-3'); scramble shRNA: CCTAAGGTTAAGTCGCCCTCG (5'-3'). These sequences were cloned into the pLKO.1-shCK-IRES-GFP plasmid. Polyethylenimine transfection was adopted for lentivirus assembly in HEK 293T cells, with pLKO.1-shACSL4-IRES-GFP plasmids (12 μg) and helper plasmids VSVG (1 μg) and Δ8.9 (3 μg) per 10 cm dish. The supernatant was collected between 24 and 48 h following transfection. The supernatant was mixed with fresh DMEM CM at a 1:1 ratio, with the addition of polybrene (8 μg/ml), and was used to treat the Ishikawa cell line for 12 h. The GFP-positive cells were sorted by FACS, and the knockdown efficiency was checked by Western blotting.

In vitro implantation model

Cell adhesion assays were conducted following a previously described protocol (33). Ishikawa cells stably transfected with ACSL4 shRNA expression plasmid or empty plasmid were grown on 96-well plates, and the experiment was conducted until the cells formed a confluent monolayer. JAR cells were stained with the fluorescent carbocyanine dye Dil (Yeasen, Shanghai, China) for 2 min before the adhesion assay. The stained JAR cells were plated onto cell monolayers in 96-well plates at a density of 1×10^4/well and cocultured at 37 °C with 5% CO_2 and 90% humidity for 1 h in DMEM/F12 culture medium. Following incubation, the wells

were gently washed three times with PBS to remove nonadherent JAR cells. Adhesion rate of JAR cells = (the average number of JAR cells in three visual fields of one well/area of a visual field * the bottom area of one well/total JAR cells added to one well) × 100%. The images were captured with a fluorescence microscope, and representative images are shown.

Treatment of progesterone

Ishikawa cells were plated and cultured in phenol red-free DMEM/F12 supplemented with 10% charcoal-stripped FBS at 37◦C and 5% CO2 for 24 h. After starvation in serum-free medium for 24 h, the cells were treated with 10^{-6} M progesterone (Sigma-Aldrich, USA) in phenol red-free DMEM/F12 supplemented with 10% charcoal-stripped FBS for 0h, 8h, 24h, 48h. Cells were harvested and total RNA and protein were extracted for the expression analysis of ACSL4 and GAPDH. All experiments were repeated three times.

Statistical analysis

Statistical analysis was performed with the use of SPSS 19.0. Student's t-test was applied to determine the significance of quantitative data. The data are expressed as the mean ± standard deviation (M± SD), and a p value < 0.05 was considered significant.

Results

Quantitative proteomic analysis of endometrial proteins by iTRAQ

iTRAQ-based quantitative proteomic analysis was performed to profile the protein divergence between prereceptive and receptive endometrium (Supplemental Figure 1) (26). Four prereceptive and four receptive endometrial protein samples were labeled with iTRAQ tags and analyzed by LC–MS/MS. A total of 3874 proteins (Supplemental Table 2) (26) were identified as differentially expressed from 18729 peptides (Supplemental Table 3) (26) using a 1% false discovery rate (FDR) as a cutoff in all eight samples. The obtained results showed a wide coverage of the protein identification in this iTRAQ analysis (Supplemental Table 4) (26):

1) 118 large proteins (molecular weight >200 kDa) and 166 small proteins (molecular weight <10 kDa) were identified; 2) 160 strong alkaline (calculated P.I.>10) and 352 strong acidic (calculated P.I.<5) proteins were identified; 3) 24.21% of proteins (725 among 2995 with available GO-cellular component information) were annotated as membrane proteins with high hydrophobicity. Using a cutoff of fold change > 1.5 and $p < 0.05$, 173 DEPs between prereceptive and receptive endometrium (Supplemental Table 5) (26) were identified. Among them, 111 proteins were upregulated and 62 were downregulated in the receptive endometrium. Hierarchical clustering displayed variations in the expression of DEPs among the detected samples and homogeneity within groups (Supplemental Figure 2) (26). The RAW data and protein/peptide identifications of iTRAQ-based proteomics have been deposited to the ProteomeXchange Consortium (http://proteomecentral.proteomexchange.org) via the iProX partner repository with the dataset identifier PXD039161.

Identification of concordant DEPs with consistent trends at both the mRNA and protein levels

Gene expression regulation and protein function are often coupled and coordinated; thus, verifying the consistency of mRNA and protein changes is very powerful for confirming the activation or inhibition of a gene/protein. Our previous RNA-seq analysis identified 2372 differentially expressed genes (DEGs) between the prereceptive and receptive endometrium(15). We subsequently mapped 140 annotated DEPs among 173 DEPs identified by iTRAQ analysis to 2372 DEGs and identified 63 DEPs with consistent trends at both the mRNA and protein levels, which were named “concordant DEPs” (Table 1). We performed a literature search to determine whether the expression and function of these proteins/genes in the endometrium had previously been described. The DEPs whose differential expression was only shown at the transcriptome or proteome level but without specific biological validation were excluded from our search. The obtained results showed that 26 of the 63 concordant DEPs

had been studied in the endometrium, involving their expression in the receptive endometrium and abnormal expression in certain pathological states (endometriosis, RIF), roles and regulatory mechanisms in decidualization and endometrial receptivity (Table 1). Six proteins (MUC1, SA00A10, PTGS1, TNC, PGR and MMP11) had previously been shown to have identical expression changes between the prereceptive and receptive phases, supported by detailed cellular and molecular experiments at the protein level, serving as a strong validation of the iTRAQ proteomics results.

Gene ontology (GO) and pathway analysis of concordant DEPs

To clarify the biological processes associated with protein expression changes during the window of implantation, we performed Gene Ontology (GO) and pathway analysis on the concordant DEPs. Enriched GO terms are shown in Figure 1A and arranged according to biological processes, cellular components and molecular function. In the cellular component assay, up to 50% of concordant DEPs were localized to the membrane, indicating the powerful detection of membrane proteins by the iTRAQ method. The molecular functions of core DEPs were mainly related to binding and catalytic activities. The enriched biological processes were mainly involved in development, response to stimulus, adhesion and regulation. Of note, the reproduction process was also significantly enriched. Pathway analysis of concordant DEPs was performed using KEGG. The enriched pathways are shown in Figure 1B. Most pathways were related to metabolic processes, including energy, lipid, nucleotide and vitamin metabolism. Several pathways related to signaling, cellular community, transport and catabolism were also enriched.

Protein–protein interaction (PPI) network analysis of concordant DEPs

Proteins always perform their functions through interactions with each other (65). Therefore, the PPI network based on enriched pathways and corresponding DEPs was constructed using the OmicsBean platform to find the hub proteins. The network model was generated using the

Cytoscape project based on information in 3 levels of functional analysis: fold-change of the DEPs, protein–protein interactions and KEGG pathway enrichment. An integrated network is shown in Figure 1C. The obtained data clearly show that most of the DEPs were upregulated in fatty acid metabolism, purine metabolism, caffeine metabolism, and the peroxisome and PPAR signaling pathways, while the DEPs in ECM-receptor interaction and protein digestion and absorption were downregulated. Connections of the nodes were calculated to screen the hub proteins. The top 5 hub proteins (connections ≥5), ACSL4, ACSL5, COL1A1, PTGS1 and PLA2G4F, were identified in the PPI network (Figure 1C, D). ACSL4 had the most connections and is thus considered to be an essential hub protein that may play important roles in the establishment of endometrial receptivity. This protein was involved in more than one KEGG pathway, including fatty acid metabolism and the peroxisome and PPAR signaling pathways.

Temporospatial expression and cellular localization of ACSL4 in the human endometrium and its abnormal expression in RIF

ACSL4 was selected to illustrate the iTRAQ results. Real-time RT–PCR and Western blot analysis were performed to detect the expression of ACSL4 in the endometrium. As shown in Figure 2A,B, both the mRNA and protein expression levels of ACSL4 were significantly upregulated in the LH+7 endometrium compared to the LH+2 endometrium. The immunohistochemistry results further verified the higher expression of ACSL4 in LH+7 endometrium (Figure 2C,D). We isolated epithelial cells and stromal cells from the endometrium and detected the expression of ACSL4. ACSL4 was mainly expressed in epithelial cells, and the expression level in stromal cells was very low (Figure 2E), which was consistent with the immunohistochemistry results (Figure 2C,D).

We also detected the expression of ACSL4 in endometrial samples from patients with RIF by Western blot. The obtained results showed that the protein expression of ACSL4 was significantly downregulated in RIF patients (Figure 2F), indicating its potential involvement in

the process of embryo implantation.

ACSL4 knockdown impaired endometrial epithelial cell adhesive capacity and downregulated the expression of HOXA10, COX2 and LIF

The shRNA eukaryotic expression plasmid targeting ACSL4 was successfully constructed and stably transfected into endometrial epithelial Ishikawa cells (shACSL4), which could significantly reduce the expression of ACSL4 compared with the empty plasmid transfected group (shCK) (Figure 3A, Supplemental Figure 3) (26).

The potential role of ACSL4 in cell adhesion during embryo implantation was determined using an in vitro implantation model composed of trophoblast JAR cells and Ishikawa cells stably transfected with ACSL4 shRNA. The adherent JAR cells were observed by fluorescent staining, and the adhesion rates were calculated. As shown in Figure 3B and Supplemental Figure 4 (26), knockdown of ACSL4 significantly decreased the adhesion rate of JAR cells to Ishikawa cells compared with the control groups ($P < 0.001$). This finding drove us to illustrate the molecular basis underlying the defective adhesion after ACSL4 knockdown. Next, we detected the expression of the potential endometrial receptivity markers HOXA10, COX2 and LIF by Western blotting. The obtained results demonstrated that the protein levels of all three genes were significantly decreased after knockdown of ACSL4 (Figure 3C, Supplemental Figure 5) (26).

Effect of progesterone on the expression of ACSL4

Progesterone is the major driver of epithelial differentiation during the acquisition of endometrial receptivity. Therefore, we determined the impact of progesterone on ACSL4 expression in Ishikawa cells. As shown in Figure 4, both the mRNA and the protein levels of ACSL4 were significantly up-regulated by progesterone.

Discussion

In this study, we first compared the protein expression changes between the LH+2 and LH+7

endometria using iTRAQ, a gel-free quantitative proteomic approach, and a total of 173 DEPs were identified. Compared with previous 2-DE-based proteomic assays, iTRAQ shows a more powerful resolution to detect membrane, strong acid, strong alkalic, excessively large and excessively small proteins. As shown in Supplemental Table 1 (26), gel-based proteomic analysis performed on LH+2 and LH+7 endometria identified 9, 16, 31 and 32 DEPs, respectively. However, no commonly changed proteins were identified among these four studies. Only 8 DEPs overlapped between Domínguez's and Li's studies (17, 18). After the removal of redundancy, a total of 80 DEPs were identified by these four studies. In comparison with the current study, only 4 proteins (APOC1, RCN1, S100A10, and TAGLN) were common. The surprising discrepancy in the numbers of DEPs between previous studies and our own was interpreted as being due to the different sensitivities of the proteomic approaches (gel-based vs. gel-free, MALDI-MS vs. LC–MS, etc.) as well as genuine differences in proteins produced in the different tissue samples (fertility, exact timing of samples, age, etc.).

We compared Chen's data on proliferative and midsecretary endometrium produced with the label-free method (21) and ours and found that 52 proteins (52/173, 30.06%) overlapped between the two lists. Among the 5 hub proteins (Figure 1), the top four (ACSL4, ACSL5, COL1A1 and PTGS1) were included in the overlapping list. Although the samples were from different phases (proliferative/mid-secretory vs. early-secretory/mid-secretory), these two studies showed high percentages of overlapping DEPs, which may be attributed to similar protein preparations and high-throughput proteomic strategies (gel-free and LC–MS).

Proteomics and transcriptomics are complementary methods that provide diverse but comparable views, which will improve our understanding of the complexity of endometrial receptivity, including the identification of key biomarkers. Using an integrated analysis of proteomic data with previous transcriptomic data (15), 63 concordant DEPs for endometrial receptivity and their associated regulatory network were investigated for the first time in this

study. Five DEPs, namely, ACSL4, ACSL5, COL1A1, PTGS1 and PLA2G4F, located in the central position in the PPI network were identified as hub proteins.

ACSL4 is an isozyme of the long-chain fatty-acid-coenzyme A ligase family with a high substrate preference for arachidonic acid. ACSL4 is abundantly expressed in steroidogenic tissues, and previous data suggest that ACSL4 plays a role in regulating prostaglandin and progesterone synthesis. In smooth muscle cells, the inhibition of ACSL4 with rosiglitazone or triacsin C increased PGE2 release, while in breast cancer cells, the knockdown of ACSL4 decreased the production of PGE2 (66-68). The knockdown of ACSL4 in Leydig cells of the testis decreases progesterone synthesis (69). Heterozygous ACSL4 deficiency impairs the progression of pregnancy because of an abnormal uterus with polycysts and the accumulation of uterine prostaglandins (37).

Our study showed that ACSL4 was mainly localized in endometrial epithelial cells, and its expression was significantly increased during the window of implantation but abnormally decreased in RIF patients, suggesting its potential roles in endometrial receptivity and embryo implantation. ACSL4 was positively responded to progesterone (Figure 4), suggesting it was a potential mediator of progesterone regulation on epithelial differentiation during the acquisition of endometrial receptivity. The study using an in vitro implantation model showed that knockdown of ACSL4 significantly reduced the adhesion rate of JAR cells to epithelial cells, which may be mediated by downregulation of the essential regulators of endometrial receptivity, HOXA10, COX2 and LIF. HOXA10 is a transcription factor of the homeobox gene that is mainly expressed in the endometrium and is related to embryo implantation (70). HOXA10 plays key regulatory roles in the expression of endometrial receptivity markers such as estrogen receptor, pinopodes, integrin αnβ3, and insulin growth factor binding protein 1 (IGFBP-1) (70). Hoxa10 -/- mice can produce high-quality normal embryos; however, due to defects in endometrial receptivity and decidualization, embryo implantation cannot occur,

resulting in infertility (71). COX2 is the rate-limiting enzyme for prostaglandin biosynthesis, whose transcription is upregulated by embryonic-derived IL-1β, resulting in increased prostaglandin biosynthesis in stromal cells at the implantation site, which is a central element in the establishment of endometrial receptivity (72). Deletion of the Cox2 gene in mice leads to various reproductive disorders, including ovulation, fertilization, implantation and decidualization, indicating the essential roles of prostaglandins produced by COX2 in female reproductive processes (73). LIF is a secretory glycoprotein belonging to the interleukin (IL)-6 superfamily and is known to play a major role in endometrial receptivity (70). During the window of implantation, LIF promotes the development of pinopodes and supports blastocyst attachment and invasion and the decidualization process (74). The expression of HOXA10, COX2 and LIF in RIF patients was abnormally downregulated (70, 75), which is consistent with ACSL4 (Figure 2F, 3C), indicating the potential etiological effects of ACSL4 on RIF. These results suggest that ACSL4 plays an important role in the regulation of endometrial receptivity and embryo implantation. ACSL4 may potentially serve as a novel marker of endometrial receptivity.

Epigenetic repression of COL1A1 resulted in increased endometrial fibrosis in endometriosis, indicating its involvement in endometriosis development (64). PTGS1 is one of the rate-limiting enzymes in PG biosynthesis. It is expressed in the epithelial cells of the endometrium and modulates the preparation of the uterus for interaction with an embryo (76). ACSL5 and PLA2G4F have not been detected or studied in the endometrium. Further investigation of the expression patterns and diverse functions of these hub proteins will provide insights into the detailed mechanisms of endometrial receptivity and the identification of potential biomarkers for implantation.

Taken together, our study provides the first multidimensional collection of a set of proteins that may be potentially involved in the regulation of endometrial receptivity. In

addition, these results open a new avenue for future studies aimed at discovering novel therapeutic targets for pregnancy-related diseases, such as RIF, and improving embryo implantation in IVF treatments.

Acknowledgements

We thank Dr Wei Ding, from Shanghai Omicsspace Bioteh CO., LTD, for his kind help for proteomics assay and bioinformatics.

Data Availability

Original data generated and analyzed during this study are included in this published article or in the data repositories listed in References.

References

1. Cha J, Sun X, Dey SK. Mechanisms of implantation: strategies for successful pregnancy. *Nat Med.* 2012;18(12):1754-1767.
2. Achache H, Revel A. Endometrial receptivity markers, the journey to successful embryo implantation. *Hum Reprod Update.* 2006;12(6):731-746.
3. Bui AH, Timmons DB, Young SL. Evaluation of endometrial receptivity and implantation failure. *Curr Opin Obstet Gynecol.* 2022;34(3):107-113.
4. Ledee-Bataille N, Lapree-Delage G, Taupin JL, Dubanchet S, Frydman R, Chaouat G. Concentration of leukaemia inhibitory factor (LIF) in uterine flushing fluid is highly predictive of embryo implantation. *Hum Reprod.* 2002;17(1):213-218.
5. Amjadi F, Zandieh Z, Mehdizadeh M, et al. The uterine immunological changes may be responsible for repeated implantation failure. *J Reprod Immunol.* 2020;138:103080.
6. Lessey BA. Assessment of endometrial receptivity. *Fertil Steril.* 2011;96(3):522-529.
7. Altmae S, Esteban FJ, Stavreus-Evers A, et al. Guidelines for the design, analysis and interpretation of 'omics' data: focus on human endometrium. *Hum Reprod Update.* 2014;20(1):12-28.
8. Carson DD, Lagow E, Thathiah A, et al. Changes in gene expression during the early to mid-luteal (receptive phase) transition in human endometrium detected by high-density microarray screening. *Mol Hum Reprod.* 2002;8(9):871-879.
9. Borthwick JM, Charnock-Jones DS, Tom BD, et al. Determination of the transcript profile of human

endometrium. *Mol Hum Reprod.* 2003;9(1):19-33.
10. Kao LC, Tulac S, Lobo S, et al. Global gene profiling in human endometrium during the window of implantation. *Endocrinology.* 2002;143(6):2119-2138.
11. Haouzi D, Mahmoud K, Fourar M, et al. Identification of new biomarkers of human endometrial receptivity in the natural cycle. *Hum Reprod.* 2009;24(1):198-205.
12. Mirkin S, Arslan M, Churikov D, et al. In search of candidate genes critically expressed in the human endometrium during the window of implantation. *Hum Reprod.* 2005;20(8):2104-2117.
13. Riesewijk A, Martin J, van Os R, et al. Gene expression profiling of human endometrial receptivity on days LH+2 versus LH+7 by microarray technology. *Mol Hum Reprod.* 2003;9(5):253-264.
14. Talbi S, Hamilton AE, Vo KC, et al. Molecular phenotyping of human endometrium distinguishes menstrual cycle phases and underlying biological processes in normo-ovulatory women. *Endocrinology.* 2006;147(3):1097-1121.
15. Hu S, Yao G, Wang Y, et al. Transcriptomic changes during the pre-receptive to receptive transition in human endometrium detected by RNA-Seq. *J Clin Endocrinol Metab.* 2014;99(12):E2744-2753.
16. DeSouza L, Diehl G, Yang EC, et al. Proteomic analysis of the proliferative and secretory phases of the human endometrium: protein identification and differential protein expression. *Proteomics.* 2005;5(1):270-281.
17. Dominguez F, Garrido-Gomez T, Lopez JA, et al. Proteomic analysis of the human receptive versus non-receptive endometrium using differential in-gel electrophoresis and MALDI-MS unveils stathmin 1 and annexin A2 as differentially regulated. *Hum Reprod.* 2009;24(10):2607-2617.
18. Li J, Tan Z, Li M, Xia T, Liu P, Yu W. Proteomic analysis of endometrium in fertile women during the prereceptive and receptive phases after luteinizing hormone surge. *Fertil Steril.* 2011;95(3):1161-1163.
19. Rai P, Kota V, Sundaram CS, Deendayal M, Shivaji S. Proteome of human endometrium: Identification of differentially expressed proteins in proliferative and secretory phase endometrium. *Proteomics Clin Appl.* 2010;4(1):48-59.
20. Parmar T, Gadkar-Sable S, Savardekar L, et al. Protein profiling of human endometrial tissues in the midsecretory and proliferative phases of the menstrual cycle. *Fertil Steril.* 2009;92(3):1091-1103.
21. Chen Q, Zhang A, Yu F, et al. Label-free proteomics uncovers energy metabolism and focal adhesion regulations responsive for endometrium receptivity. *J Proteome Res.* 2015;14(4):1831-1842.
22. Bissonnette L, Drissennek L, Antoine Y, et al. Human S100A10 plays a crucial role in the acquisition of the endometrial receptivity phenotype. *Cell Adh Migr.* 2016;10(3):282-298.
23. Garrido-Gomez T, Quinonero A, Antunez O, et al. Deciphering the proteomic signature of human endometrial receptivity. *Hum Reprod.* 2014;29(9):1957-1967.
24. Manohar M, Khan H, Sirohi VK, et al. Alteration in endometrial proteins during early- and mid-secretory phases of the cycle in women with unexplained infertility. *PLoS One.* 2014;9(11):e111687.

25. Chen JI, Hannan NJ, Mak Y, et al. Proteomic characterization of midproliferative and midsecretory human endometrium. *J Proteome Res.* 2009;8(4):2032-2044.
26. Hu S, Sun Z, Li B, et al. Data from: iTRAQ-based proteomic analysis unveils ACSL4 as a novel potential regulator of human endometrial receptivity. *figshare.* Deposited 3 January 2023. https://doi.org/10.6084/m9.figshare.c.6365799.v2
27. Latosinska A, Vougas K, Makridakis M, et al. Comparative Analysis of Label-Free and 8-Plex iTRAQ Approach for Quantitative Tissue Proteomic Analysis. *PLoS One.* 2015;10(9):e0137048.
28. Pottiez G, Wiederin J, Fox HS, Ciborowski P. Comparison of 4-plex to 8-plex iTRAQ quantitative measurements of proteins in human plasma samples. *J Proteome Res.* 2012;11(7):3774-3781.
29. Marianowski P, Szymusik I, Malejczyk J, Hibner M, Wielgos M. Proteomic analysis of eutopic and ectopic endometriotic tissues based on isobaric peptide tags for relative and absolute quantification (iTRAQ) method. *Neuro Endocrinol Lett.* 2013;34(7):717-721.
30. Meng Y, Guo Y, Qian Y, et al. Effects of GnRH antagonist on endometrial protein profiles in the window of implantation. *Proteomics.* 2014;14(20):2350-2359.
31. Xu J, Shao X, Wei Y, Xu F, Wang H. iTRAQ Proteomic Analysis Reveals That Metabolic Pathways Involving Energy Metabolism Are Affected by Tea Tree Oil in Botrytis cinerea. *Front Microbiol.* 2017;8:1989.
32. Wang Y, Hu S, Yao G, et al. A Novel Molecule in Human Cyclic Endometrium: LncRNA TUNAR Is Involved in Embryo Implantation. *Front Physiol.* 2020;11:587448.
33. Guo C, Kong F, Lv Y, Gao N, Xiu X, Sun X. CDC20 inhibitor Apcin inhibits embryo implantation in vivo and in vitro. *Cell Biochem Funct.* 2020;38(6):810-816.
34. Vargas MF, Tapia-Pizarro AA, Henriquez SP, et al. Effect of single post-ovulatory administration of levonorgestrel on gene expression profile during the receptive period of the human endometrium. *J Mol Endocrinol.* 2012;48(1):25-36.
35. Yamagata Y, Nishino K, Takaki E, et al. Genome-wide DNA methylation profiling in cultured eutopic and ectopic endometrial stromal cells. *PLoS One.* 2014;9(1):e83612.
36. Zeng H, Fu Y, Shen L, Quan S. Integrated Analysis of Multiple Microarrays Based on Raw Data Identified Novel Gene Signatures in Recurrent Implantation Failure. *Front Endocrinol (Lausanne).* 2022;13:785462.
37. Cho YY, Kang MJ, Sone H, et al. Abnormal uterus with polycysts, accumulation of uterine prostaglandins, and reduced fertility in mice heterozygous for acyl-CoA synthetase 4 deficiency. *Biochem Biophys Res Commun.* 2001;284(4):993-997.
38. Aplin JD. MUC-1 glycosylation in endometrium: possible roles of the apical glycocalyx at implantation. *Hum Reprod.* 1999;14 Suppl 2:17-25.
39. Meseguer M, Pellicer A, Simon C. MUC1 and endometrial receptivity. *Mol Hum Reprod.*

1998;4(12):1089-1098.
40. Zhu YY, Wu Y, Chen ST, et al. In situ Synthesized Monosodium Urate Crystal Enhances Endometrium Decidualization via Sterile Inflammation During Pregnancy. *Front Cell Dev Biol.* 2021;9:702590.
41. Catalano RD, Wilson MR, Boddy SC, Jabbour HN. Comprehensive expression analysis of prostanoid enzymes and receptors in the human endometrium across the menstrual cycle. *Mol Hum Reprod.* 2011;17(3):182-192.
42. Smith WL, Langenbach R. Why there are two cyclooxygenase isozymes. *J Clin Invest.* 2001;107(12):1491-1495.
43. Yang H, Zhou Y, Edelshain B, Schatz F, Lockwood CJ, Taylor HS. FKBP4 is regulated by HOXA10 during decidualization and in endometriosis. *Reproduction.* 2012;143(4):531-538.
44. Al-Gubory KH, Arianmanesh M, Garrel C, Fowler PA. The conceptus regulates tryptophanyl-tRNA synthetase and superoxide dismutase 2 in the sheep caruncular endometrium during early pregnancy. *Int J Biochem Cell Biol.* 2015;60:112-118.
45. Albayrak IG, Azhari F, Colak EN, et al. Endometrial gene expression profiling of recurrent implantation failure after in vitro fertilization. *Mol Biol Rep.* 2021;48(6):5075-5082.
46. Bastu E, Demiral I, Gunel T, et al. Potential Marker Pathways in the Endometrium That May Cause Recurrent Implantation Failure. *Reprod Sci.* 2019;26(7):879-890.
47. Zhao Y, Garcia J, Kolp L, Cheadle C, Rodriguez A, Vlahos NF. The impact of luteal phase support on gene expression of extracellular matrix protein and adhesion molecules in the human endometrium during the window of implantation following controlled ovarian stimulation with a GnRH antagonist protocol. *Fertil Steril.* 2010;94(6):2264-2271.
48. Konrad L, Gronbach J, Horne F, et al. Similar Characteristics of Endometrial and Endometriotic Epithelial Cells. *Reprod Sci.* 2019;26(1):49-59.
49. Pavone ME, Reierstad S, Sun H, Milad M, Bulun SE, Cheng YH. Altered retinoid uptake and action contributes to cell survival in endometriosis. *J Clin Endocrinol Metab.* 2010;95(11):E300-309.
50. Pavone ME, Malpani S, Dyson M, Bulun SE. Altered retinoid signaling compromises decidualization in human endometriotic stromal cells. *Reproduction.* 2017;154(3):207-216.
51. Ozaki R, Kuroda K, Ikemoto Y, et al. Reprogramming of the retinoic acid pathway in decidualizing human endometrial stromal cells. *PLoS One.* 2017;12(3):e0173035.
52. Horne F, Dietze R, Berkes E, et al. Impaired Localization of Claudin-11 in Endometriotic Epithelial Cells Compared to Endometrial Cells. *Reprod Sci.* 2019;26(9):1181-1192.
53. Schumann S, Buck VU, Classen-Linke I, Wennemuth G, Grummer R. Claudin-3, claudin-7, and claudin-10 show different distribution patterns during decidualization and trophoblast invasion in mouse and human. *Histochem Cell Biol.* 2015;144(6):571-585.
54. Ma S, Hirata T, Arakawa T, et al. Expression of ALDH1A Isozymes in Human Endometrium with and

without Endometriosis and in Ovarian Endometrioma. *Reprod Sci.* 2020;27(1):443-452.
55. Patterson AL, Squires EL, Hansen TR, Bouma GJ, Bruemmer JE. Gene profiling of inflammatory genes in day 18 endometria from pregnant and non-pregnant mares. *Mol Reprod Dev.* 2012;79(11):777-784.
56. Vollmer G. Expression of tenascin during carcinogenesis and involution of hormone-dependent tissues. *Biochem Cell Biol.* 1994;72(11-12):505-514.
57. Wang H, Critchley HO, Kelly RW, Shen D, Baird DT. Progesterone receptor subtype B is differentially regulated in human endometrial stroma. *Mol Hum Reprod.* 1998;4(4):407-412.
58. DeMayo FJ, Lydon JP. 90 YEARS OF PROGESTERONE: New insights into progesterone receptor signaling in the endometrium required for embryo implantation. *J Mol Endocrinol.* 2020;65(1):T1-T14.
59. Chen P, Mamillapalli R, Habata S, Taylor HS. Endometriosis Cell Proliferation Induced by Bone Marrow Mesenchymal Stem Cells. *Reprod Sci.* 2021;28(2):426-434.
60. Goffin F, Munaut C, Frankenne F, et al. Expression pattern of metalloproteinases and tissue inhibitors of matrix-metalloproteinases in cycling human endometrium. *Biol Reprod.* 2003;69(3):976-984.
61. Wang Y, Hu S, Yao G, Sun Y. Identification of HOXA10 target genes in human endometrial stromal cells by RNA-seq analysis. *Acta Biochim Biophys Sin (Shanghai).* 2021;53(3):365-371.
62. Celik O, Celik N, Ugur K, et al. Nppc/Npr2/cGMP signaling cascade maintains oocyte developmental capacity. *Cell Mol Biol (Noisy-le-grand).* 2019;65(4):83-89.
63. Kim TH, Yoo JY, Choi KC, et al. Loss of HDAC3 results in nonreceptive endometrium and female infertility. *Sci Transl Med.* 2019;11(474).
64. Zheng Y, Khan Z, Zanfagnin V, Correa LF, Delaney AA, Daftary GS. Epigenetic Modulation of Collagen 1A1: Therapeutic Implications in Fibrosis and Endometriosis. *Biol Reprod.* 2016;94(4):87.
65. Eisenberg D, Marcotte EM, Xenarios I, Yeates TO. Protein function in the post-genomic era. *Nature.* 2000;405(6788):823-826.
66. Golej DL, Askari B, Kramer F, et al. Long-chain acyl-CoA synthetase 4 modulates prostaglandin E(2) release from human arterial smooth muscle cells. *J Lipid Res.* 2011;52(4):782-793.
67. Maloberti PM, Duarte AB, Orlando UD, et al. Functional interaction between acyl-CoA synthetase 4, lipooxygenases and cyclooxygenase-2 in the aggressive phenotype of breast cancer cells. *PLoS One.* 2010;5(11):e15540.
68. Watkins PA, Ellis JM. Peroxisomal acyl-CoA synthetases. *Biochim Biophys Acta.* 2012;1822(9):1411-1420.
69. Cornejo Maciel F, Maloberti P, Neuman I, et al. An arachidonic acid-preferring acyl-CoA synthetase is a hormone-dependent and obligatory protein in the signal transduction pathway of steroidogenic hormones. *J Mol Endocrinol.* 2005;34(3):655-666.
70. Tan X, Ding J, Pu D, Wu J. Anti-phospholipid antibody may reduce endometrial receptivity during the window of embryo implantation. *J Gynecol Obstet Hum Reprod.* 2021;50(6):101912.

71. Satokata I, Benson G, Maas R. Sexually dimorphic sterility phenotypes in Hoxa10-deficient mice. *Nature.* 1995;374(6521):460-463.
72. Fazleabas AT, Kim JJ, Srinivasan S, Donnelly KM, Brudney A, Jaffe RC. Implantation in the baboon: endometrial responses. *Semin Reprod Endocrinol.* 1999;17(3):257-265.
73. Sales KJ, Jabbour HN. Cyclooxygenase enzymes and prostaglandins in pathology of the endometrium. *Reproduction.* 2003;126(5):559-567.
74. Mrozikiewicz AE, Ozarowski M, Jedrzejczak P. Biomolecular Markers of Recurrent Implantation Failure-A Review. *Int J Mol Sci.* 2021;22(18).
75. Achache H, Tsafrir A, Prus D, Reich R, Revel A. Defective endometrial prostaglandin synthesis identified in patients with repeated implantation failure undergoing in vitro fertilization. *Fertil Steril.* 2010;94(4):1271-1278.
76. Stavreus-Evers A, Koraen L, Scott JE, Zhang P, Westlund P. Distribution of cyclooxygenase-1, cyclooxygenase-2, and cytosolic phospholipase A2 in the luteal phase human endometrium and ovary. *Fertil Steril.* 2005;83(1):156-162.

Legends for Figures and Tables

Figure 1 Gene Ontology (GO), KEGG pathway and protein–protein interaction (PPI) network analyses of concordant DEPs. A) GO analysis. A bar plot was generated from the top 10 GO terms with the highest P values for biological processes, cellular component and molecular function. P <0.05 was used as a threshold to select GO terms. B) KEGG pathway analysis. P <0.05 was used as a threshold to select significant KEGG pathways. C) The PPI network model is also based on the fold change of concordant DEPs and KEGG pathway enrichment. Proteins are indicated by circles with gradient colors (red for upregulated proteins and green for downregulated proteins). Rectangles indicate KEGG pathways with gradient colors from yellow (smaller P value) to blue (bigger P value). The hub proteins are highlighted by the blue rectangle. D) Characterization of the hub proteins derived from the network model of C).

Figure 2 The expression and localization of ACSL4 in the human endometrium. A) The mRNA expression of ACSL4 in human LH+2 and LH+7 endometria by real-time RT–PCR analysis. LH+2: LH+7 = 5: 5. B) The protein expression of ACSL4 in human late proliferative (LP), early secretory (ES, LH+2) and mid-secretory (MS, LH+7) endometria by Western blot analysis. LP: ES: MS=4: 5: 5. C&D) Immunohistochemical staining of ACSL4 in proliferative endometrium (C) and receptive (LH+7) endometrium (D) (n=3). Normal rabbit IgG was used as a negative control (C-a, D-a). Scale bars for C-a, b and D-a, b were 50 μm, while for C-c, d and D-c, d were 25 μm. E) The expression of ACSL4 protein in endometrial epithelial cells (EEC, E) and stromal cells (ESC, S) from the same patients in LH + 7 phase (n = 3). F) The expression of ACSL4 in LH+7 endometria from RIF patients (RIF, n=12) and controls (CTRL, n=12) by Western blot analysis. β-actin was used as an internal control in A); GAPDH was used as an internal control for B), E) and F). *P < 0.05, ***P < 0.001

Figure 3 The potential effects of ACSL4 on human embryo implantation and expression of endometrial receptivity markers. A) The expression of ACSL4 in Ishikawa cells stably transfected with ACSL4 shRNA expression plasmid (shACSL4) and empty plasmid (shCK) (n =4). B) The adhesive capacity of Ishikawa cells to JAR cells after stable transfection with ACSL4 shRNA expression plasmid (shACSL4) and empty plasmid (shCK) (n =6). Representative fluorescence images are shown. C) The expression of HOXA10, COX2 and LIF in Ishikawa cells stably transfected with ACSL4 shRNA expression plasmid (shACSL4) and empty plasmid (shCK) (n =3). GAPDH was used as an internal control for A) and C). *P < 0.05, **P < 0.01, ***P < 0.001

Figure 4 The effect of progesterone on ACSL4 expression in ishikawa cells. A) Real time

RT-PCR detection of ACSL4 mRNA expression in ishikawa cells after 10^{-6} M progesterone treatment (n=3). β-actin was used as an internal control. B) Western blot analysis of ACSL4 protein expression in ishikawa cells after 10^{-6} M progesterone treatment (n=3). GAPDH was used as an internal control. *P < 0.05, ***P < 0.001

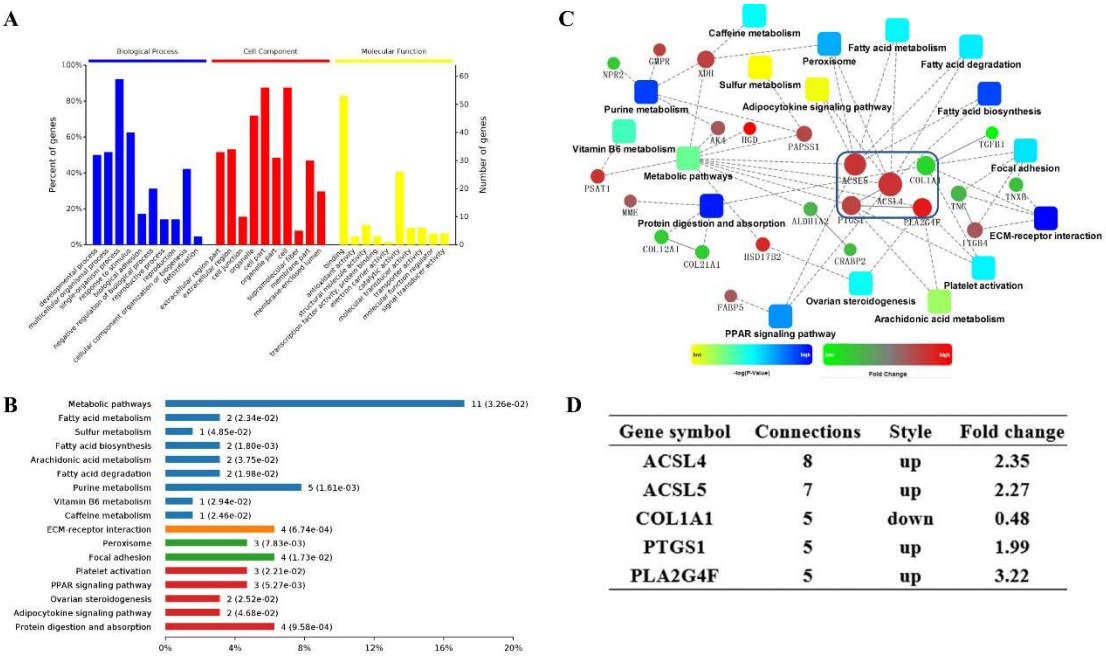

D

Gene symbol	Connections	Style	Fold change
ACSL4	8	up	2.35
ACSL5	7	up	2.27
COL1A1	5	down	0.48
PTGS1	5	up	1.99
PLA2G4F	5	up	3.22

Figure 1

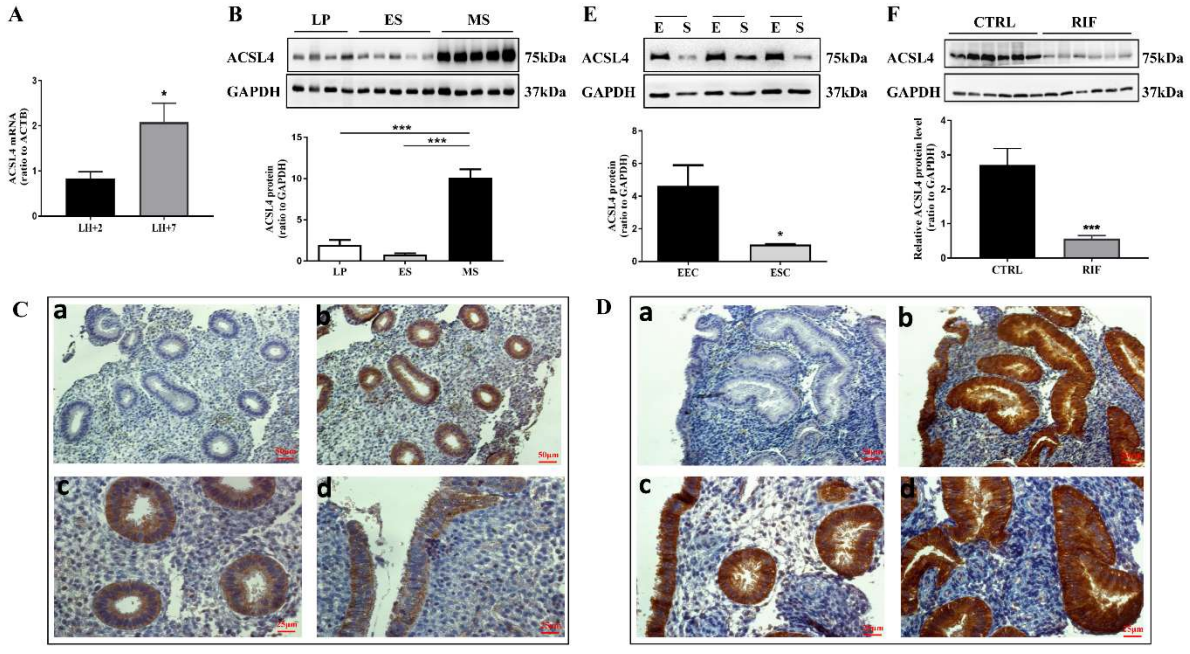

Figure 2

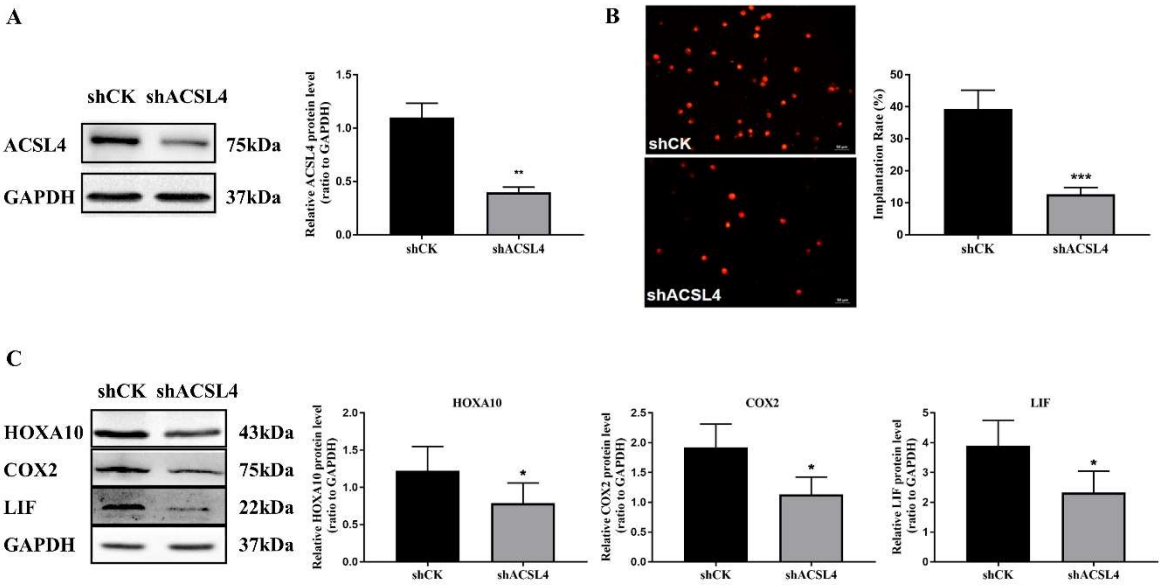

Figure 3

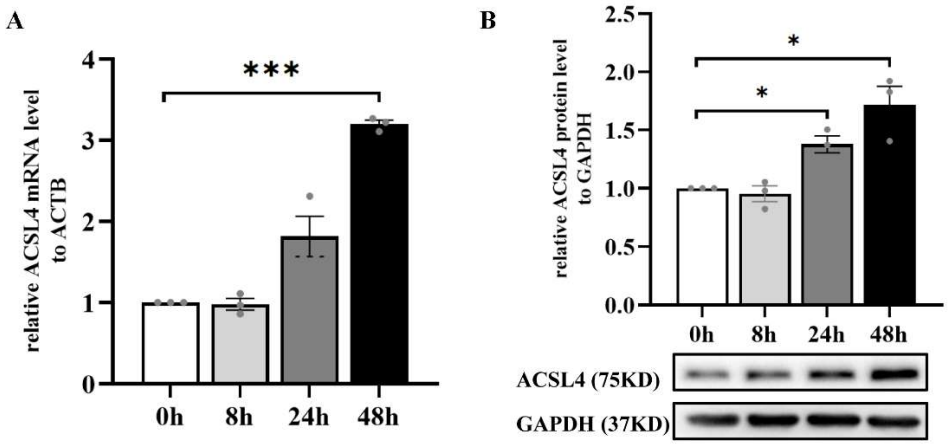

Figure 4

Table 1 Condordant DEPs identified by integrated analysis of endometrial transcriptome and proteome (LH+7 vs LH+2)

Gene symbol	Style	Protein change		mRNA change		Endometrial expression and function	References
		Fold change	P Value	Fold change	P-Value		
HGD	up	4.22	0.00102	17.68	2.98418E-18	Up-regulation of mRNA during the window of implantation	(9,10)
SLC39A14	up	4.05	0.00008	16.23	7.62591E-33	Decreased expression after administering levonorgestrel	(34)
PLA2G4F	up	3.22	0.00004	233.94	8.03211E-47	NA	
MPZL2	up	2.92	0.00182	9.35	9.17542E-31	NA	
HSD17B2	up	2.66	0.00367	22.18	9.53267E-19	Decreased expression due to DNA hypermethylation may contribute to the development of endometriosis	(35)
TPD52L1	up	2.64	0.00037	7.56	3.56331E-16	Abnormally high expression in RIF patients	(36)
PSAT1	up	2.37	0.00026	12.47	8.59565E-46	NA	
ACSL4	up	2.35	0.00044	2.46	3.24373E-09	Modulation of female fertility and uterine prostaglandin production in mouse (ACSL4 +/- model)	(37)
ACSL5	up	2.27	0.00000	6.26	3.14379E-14	NA	
FAM213A	up	2.22	0.02614	3.22	4.09757E-20	NA	
MUC1	up	2.12	0.01678	2.87	3.36315E-07	A molecular marker of endometrial receptivity; aboundant during WOI; decreased in infertile patients	(38,39)
XDH	up	2.03	0.00075	167.85	2.08519E-28	Increased expression along with decidualization in both human and mouse	(40)
S100A10	up	2.03	0.00463	9.81	4.85682E-23	Up-regulation during WOI; down-regulation in RIF patients; a regulator of endometrial receptivity by affecting migration, decidualization and apoptosis	(22)
GMPR	up	2.02	0.00526	7.59	1.54146E-19	NA	
SLC34A2	up	2.01	0.01884	6.23	3.1744E-22	NA	

NOL3	up	1.99	0.02732	3.49	1.08267E-10	NA	
PTGS1	up	1.99	0.03509	12.76	3.07578E-32	Normal fertilization but difficulty with parturition in ptgs1-/- mouse; Upregulation during WOI	(41,42)
ACPP	up	1.96	0.01671	10.89	5.85968E-37	NA	
CILP	up	1.92	0.01367	5.39	8.82455E-12	NA	
RNASET2	up	1.92	0.04935	3.80	1.48227E-09	NA	
DUOX1	up	1.90	0.01569	24.42	6.21549E-17	NA	
ANXA3	up	1.89	0.00801	3.98	1.13699E-08	NA	
PAPSS1	up	1.84	0.00004	3.19	9.32612E-12	NA	
FKBP5	up	1.83	0.00019	28.38	9.63947E-73	Knockdown of FKBP5 didn’t affect the decidualization	(43)
SNX9	up	1.79	0.00154	3.43	1.52675E-21	NA	
TAP1	up	1.76	0.02359	2.36	5.52356E-07	NA	
LPCAT3	up	1.75	0.00056	2.53	2.99139E-12	NA	
WARS	up	1.71	0.01979	2.10	5.06212E-07	Upregulation by conceptus-derived signals favorably influences implantation in ovine endometrium	(44)
PPL	up	1.65	0.01083	3.99	4.97546E-20	NA	
MVP	up	1.65	0.00012	4.78	1.13543E-27	NA	
JUP	up	1.65	0.00299	4.37	7.29343E-19	NA	
DUOXA1	up	1.61	0.01031	21.38	6.76639E-15	NA	
AK4	up	1.59	0.00121	3.36	2.70954E-13	NA	
EPS8L2	up	1.58	0.00770	2.89	1.47724E-16	NA	
MME	up	1.57	0.01449	3.69	3.45623E-11	Abnormally increased expression in RIF patients	(45,46)
ITGB4	up	1.56	0.00002	6.02	8.09331E-24	Up-regulation upon luteal support (P or P+E)	(47)
KRT19	up	1.55	0.00335	2.08	1.64959E-06	Decreased expression in the endometriotic lesions; involvement of endometriosis	(48)

FABP5	up	1.55	0.01660	5.13	4.79781E-14	Decreased expression upon decidualization; Knockdown of FABP5 induced decidualization, increased apoptosis and decreased proliferation in endometriotic stromal cells	(49-51)
CLDN7	up	1.53	0.04632	3.60	1.29374E-22	Basolateral localization in HEECs; No significant change in endometriosis; No significant difference between proliferative and secretary phases; decrease at the time of implantation in mouse and rat	(52,53)
CNN3	down	0.67	0.00665	0.43	9.51795E-09	NA	
SMC2	down	0.65	0.00782	0.36	2.49198E-12	NA	
ALDH1A2	down	0.64	0.00035	0.37	6.41202E-14	Mainly expressed in stromal cells; No significant difference between proliferative and secretary phases	(54)
MARCKSL1	down	0.64	0.00000	0.21	4.25359E-26	Decreased expression in endometrial tissue from pregnant mares	(55)
TNC	down	0.62	0.01288	0.14	6.67558E-14	Decreased expression in secretory phase; Abnormally decreased expression in RIF patients	(45,56)
CNN1	down	0.62	0.00148	0.28	7.27881E-07	NA	
APOB	down	0.61	0.02522	0.30	1.31084E-06	NA	
NUDT4	down	0.61	0.00231	0.39	2.59705E-09	NA	
PGR	down	0.60	0.00025	0.12	1.57994E-43	Decreased expression in secretory phase; master regulator of endometrial receptivity	(57,58)
CRABP2	down	0.60	0.00003	0.11	5.83703E-30	Decreased expression in endometriotic stromal cells; Ablation of CRABP2 compromises decidualization, decreases apoptosis and increases proliferation in ESC.	(49-51)
MRC2	down	0.59	0.00034	0.27	8.24373E-21	NA	
TNXB	down	0.57	0.01222	0.45	3.78261E-08	NA	
FHL2	down	0.55	0.00180	0.29	1.36887E-07	NA	
CDK1	down	0.54	0.01567	0.12	6.86178E-28	Up-regulation in endometriosis; etiological effect on endometriosis.	(59)

MMP11	down	0.54	0.00680	0.01	1.95976E-79	Down-regulation in receptive phase; play roles in the pathogenesis of endometriosis.	(60,61)
PALLD	down	0.53	0.00001	0.23	5.65502E-29	NA	
COL12A1	down	0.52	0.01415	0.14	2.66667E-22	NA	
NPR2	down	0.52	0.00004	0.14	7.94947E-47	Potential relation with of uterus development and thin endometrium	(62)
COL21A1	down	0.52	0.03448	0.22	3.22306E-09	NA	
OGN	down	0.51	0.00782	0.39	4.03474E-09	NA	
COL1A1	down	0.48	0.02662	0.30	5.06243E-16	Etiological role of increased COL1A1 expression in endometrial fibrosis; transcriptional repression of COL1A1 is critical to induce decidualization of HESC	(63,64)
ANK2	down	0.44	0.00320	0.08	6.23488E-49	NA	
CA12	down	0.39	0.00089	0.20	1.03607E-19	NA	
TGFBI	down	0.34	0.00295	0.09	1.24789E-20	Decreased expression in receptive phase	(8)